

Electron Microscopic and Physico-Chemical Studies of DNA Complexes with Synthetic Oligopeptides: Binding Specificity and DNA Compact Structures

Vengerov, Y.Y.¹, Semenov, T.E.², Surovaya, A.N.²,
Sidorova, N.Yu.², Streltsov, S.A.², Khorlin, A.A.²,
Zhuze, A.L.² and Gursky, G.V.²

¹Institute of Applied Molecular Biology
USSR Ministry of Health
Sympheropolsky blvd. 8
Moscow 113149, USSR

²Institute of Molecular Biology
USSR Academy of Sciences
Vavilov str. 32
Moscow 117984, USSR

Abstract

Binding to DNA of two synthetic peptides, Val-Thr-Thr-Val-Val-NH-NH-Dns and Thr-Val-Thr-Lys-Val-Gly-Thr-Lys-Val-Gly-Thr-Val-Val-NH-NH-Dns (where Dns is a residue of 5-dimethylaminonaphthalene-1-sulfonic acid), has been studied by circular dichroism, electron microscopy and fluorescence methods. It has been found that these two peptides can self-associate in aqueous solution as follows from the fact that concentration-dependent changes are observed in the UV absorbance and fluorescence spectra. The two peptides can bind to DNA both in self-associated and monomeric forms. The pentapeptide in the β -associated form binds more strongly to poly(dG) · poly(dC) than to poly[d(A-C)] · poly[d(G-T)] and poly(dA) · poly(dT) whereas the tridecapeptide exhibits an opposite order of preferences binding more strongly to poly[d(A-C)] · poly[d(G-T)] and poly(dA) · poly(dT) than to poly(dG) · poly(dC).

Binding is a cooperative process which is accompanied by the DNA compaction at peptide/DNA base pair ratios greater than 1. At the initial stage of the compaction process, the coalescence of DNA segments covered by bound peptide molecules leads to the formation of DNA loops stabilized by the interaction between peptide molecules bound to different DNA segments. Further increase in the peptide/DNA ratio leads to the formation of rod-like structures each consisting of two or more double-stranded DNA segments. The final stage of the compaction process involves folding of fibrillar macromolecular complexes into a globular structure containing only one DNA molecule.

Introduction

Complexes of DNA with peptides folding into α -helix or β -stranded structure may be considered as model systems for studies of the interaction between DNA and

various regulatory and structural proteins. Our previous observations have shown that some of the β -structure forming peptides bind in the minor DNA groove in a sequence-specific manner (1,2). Among these peptides, the tripeptide H-Val-Val-Val-NH-NH-Dns (TVP) has the simplest structure (Dns is a residue of 5-dimethylaminonaphthyl-1-sulfonic acid). TVP binds more strongly to poly(dG) · poly(dC) than to poly(dA) · poly(dT) (1,2). Using electron microscopy, sedimentation and optical methods, it has been demonstrated that the interaction of TVP with linear double-stranded DNA leads to the formation of a rod-like structure containing two or more DNA segments associated side by side (3). Binding of TVP to a circular supercoiled DNA induces intramolecular DNA compaction and formation of compact ring-shaped particles - "triple rings" (4).

In this paper we present the results of physico-chemical and electron microscopic studies of complexes composed of DNA and synthetic peptides, H-Val-Thr-Thr-Val-Val-NH-NH-Dns (PNP) and H-Thr-Val-Thr-Lys-Val-Gly-Thr-Lys-Val-Gly-Thr-Val-Val-NH-NH-Dns (TDP). These two peptides prepared according to the general liquid phase peptide synthesis procedure with modifications described elsewhere (5,6) contain identical chemical groups at their C-termini. The experiments described below show that the two peptides bind to DNA preferentially in a self-associated form and exhibit binding preferences for certain base pair sequences on DNA. The conformational investigations performed by means of circular dichroism spectroscopy show that these two peptides assume an ordered β -like conformation upon binding to DNA. The electron microscopy studies demonstrate that they can induce a two-stage intramolecular compaction of DNA. At the first stage of the compaction process the rod-like particles are formed which are similar in their appearance to TVP-DNA complexes (3). At the second stage, the rod-shaped particles are packaged into dense globules. The ability of peptide-DNA complexes to form condensed, highly organized structures could have important bearing for DNA packing in virus particles and eukaryotic cells.

Materials and Methods

The peptides H-Val-Thr-Thr-Val-Val-NH-NH-Dns (PNP) and H-Thr-Val-Thr-Lys-Val-Gly-Thr-Lys-Val-Gly-Thr-Val-Val-NH-NH-Dns (TDP) were synthesized as described in (5,6). Calf thymus DNA was purchased from "Sigma" (USA). The linearized plasmid pBR322 DNA was kindly donated by Dr. R. Sh. Beabealashvili.

Poly(dA) · poly(dT) and poly(dG) · poly(dC) were obtained from "PL Biomedicals" (USA), poly[d(A-C)] · poly[d(G-T)] was purchased from "Boehringer Mannheim GmbH" (FRG). All polynucleotides were used as supplied, without further purification. All polynucleotide solutions were dialyzed for 6 h against 1 mM Na-cacodylate buffer (pH 7.0) in the presence of 1 mM EDTA and then dialyzed for 48 h against 1 mM Na-cacodylate buffer (pH 7.0) in the absence of EDTA.

DNA complexes with TDP and PNP were prepared by direct mixing at 20°C of aliquots of peptide solution in methanol (concentration $1 \cdot 10^{-3}$ M) and DNA solution in 1 mM Na-cacodylate buffer (pH 7.0). All solutions contained 10% (v/v) of methanol.

s observations have shown the minor DNA groove in a s, the tripeptide H-Val-Val- is a residue of 5-dimethyl- ngly to poly(dG) · poly(dC) oscopy, sedimentation and raction of TVP with linear ke structure containing two nding of TVP to a circular tion and formation of com-

l and electron microscopic eptides, H-Val-Thr-Thr- -Val-Gly-Thr-Lys-Val-Gly- prepared according to the h modifications described C-termini. The experiments NA preferentially in a self- ain base pair sequences on neans of circular dichroism rdered β -like conformation demonstrate that they can At the first stage of the com- similar in their appearance aped particles are packaged omplexes to form condensed, g for DNA packing in virus

NP) and H-Thr-Val-Thr- s (TDP) were synthesized from "Sigma" (USA). The Dr. R. Sh. Beabealashvili.

ned from "PL Biomedicals" n "Boehringer Mannheim without further purification. 1 mM Na-cacodylate buffer d for 48 h against 1 mM Na-

ct mixing at 20°C of aliquots and DNA solution in 1 mM 10% (v/v) of methanol.

Since equilibria between various aggregate forms of PNP and TDP in aqueous solution are attained for a long time (2,6), the DNA-peptide mixtures were incubated at 4°C for 48 h and at room temperature for 4 h and thereupon measurements were done.

The UV spectra were recorded with a Cary spectrophotometer (USA) using 0.1 cm, 0.5 cm and 1.0 cm pathlength cells. The CD spectra of the peptides and nucleic acids were recorded with a Jobin-Yvon Mark III dichrograph (France). Fluorescence measurements were carried out with an Aminco SPF-1000 CS (USA) instrument.

Electron microscopic specimens were prepared as follows. A 10 μ l drop of the corresponding DNA-peptide mixture was applied to the electron microscopic grid covered with collodion film. The DNA concentration in all preparations was about $1.6 \cdot 10^{-5}$ M (base pairs) whereas the concentrations of peptides varied from $1 \cdot 10^{-7}$ M to $5 \cdot 10^{-4}$ M. The preparations were contrasted either by shadowing with platinum-palladium or by uranyl acetate staining. Sometimes stained preparations were additionally shadowed.

All samples were analyzed with a JEM-100 CX ("JEOL", Japan) electron microscope at magnifications of 5000-50000 and contour lengths of DNA molecules were measured on the microphotographs with final magnifications of $50000 \times$ using a digitizer from a Hewlett-Packard computer.

Results

Interaction of PNP and TDP with DNA and Synthetic Polynucleotides

The shapes of the UV absorption and fluorescence spectra obtained for aqueous solutions of PNP and TDP undergo changes when peptide concentrations are increased from $1 \cdot 10^{-7}$ M to $1 \cdot 10^{-5}$ M. These spectral changes are similar to those observed earlier for aqueous solutions of TVP (2). The existence of concentration-dependent changes in the absorption and fluorescence spectra of PNP, TDP and TVP reflects the fact that these oligopeptides can self-associate in aqueous solution and form aggregates of different sizes that are in concentration-dependent equilibrium with each other and with monomers.

The interaction of oligopeptides with nucleic acids can be followed by UV absorbance, fluorescence and CD measurements. The addition of DNA to an oligopeptide solution induces changes in the absorption and fluorescence spectra. The nature and the magnitude of these changes are different for complexes formed by non-associated and self-associated oligopeptide species with DNA. At low concentrations of PNP (or TDP) ($C = 1 \cdot 10^{-6}$ M), when each oligopeptide exists in solution predominantly in the monomeric form, the addition of DNA results in a slight decrease in the amplitude of the long wavelength absorbance band with a maximum at about 330 nm. The binding is also accompanied by an increase in the magnitude of fluorescence polarization as well as by small changes in the intensity of fluorescence. The difference absorption spectra obtained by subtracting the spectra of DNA from the spectra of oligopeptide-DNA mixtures generally resemble the corresponding spectra

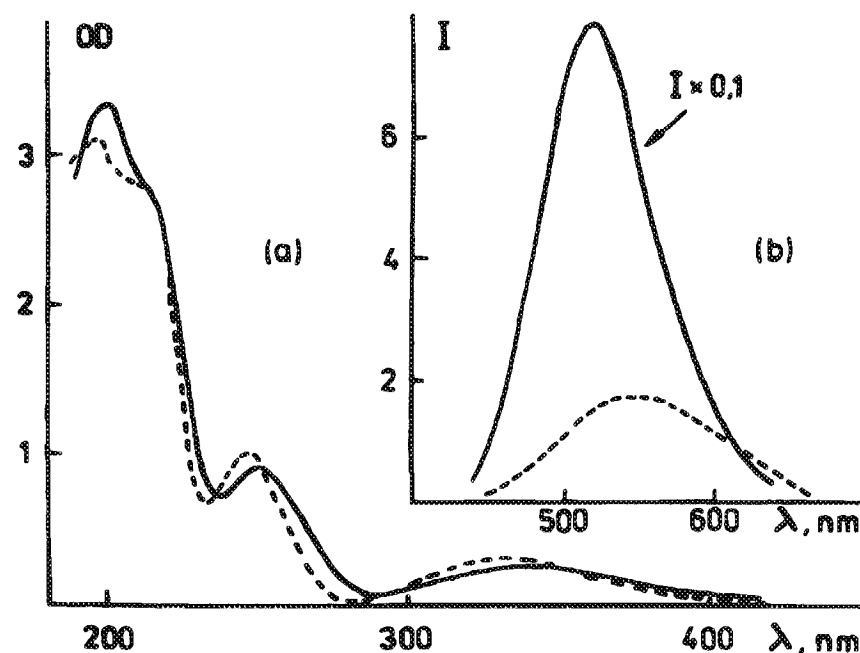


Figure 1: Changes observed in the absorption and fluorescence spectra of PNP upon binding to calf thymus DNA. (a) Absorption spectrum of free pentapeptide (---) and difference absorption spectrum obtained by subtracting the spectrum of naked DNA from the spectrum of PNP-DNA complex (—). (b) Fluorescence emission spectra (uncorrected) of free PNP (---). Fluorescence emission was excited at 380 nm. Emission and excitation slits were 10 nm. Concentration of peptide was $1 \cdot 10^{-4}$ M. DNA concentration was $1.25 \cdot 10^{-4}$ M (base pairs). Experiments were conducted at 20°C in 0.001 M Na-cacodylate buffer (pH 7.0) in the presence of 10% (v/v) methanol.

obtained for free oligopeptides, despite some minor differences in the positions of the maxima and in the amplitudes. A similar conclusion can be drawn from the comparison of the fluorescence spectra obtained for free oligopeptides and oligopeptide-DNA mixtures at an input peptide/DNA base pair ratio (2 C/P) of about $1 \cdot 10^{-2}$.

The difference absorption spectra obtained at higher concentrations, when self-associated species of PNP (or TDP) are present in solution, are shown in Figure 1 and Figure 2 for complexes with PNP and TDP, respectively. These difference spectra closely resemble those described earlier for TVP-DNA complexes (2). In all cases, the binding of self-associated peptide species to DNA is accompanied by a red-shift in the position of the absorbance band maximum at about 330 nm and by a shift in the position of a maximum in the fluorescence spectrum towards shorter wavelengths. For the sake of comparison, in Figure 1 and Figure 2 the absorption and fluorescence spectra of free PNP and TDP, respectively, are presented. The fluorescence intensity per mole of PNP (or TDP) is greatly enhanced on binding to DNA.

The CD spectra of peptide-DNA complexes as well as the spectra of PNP and TDP in the absence of DNA are shown in Figure 3 and Figure 4, respectively. The CD spectra recorded for aqueous solutions of PNP and TDP show negative bands near

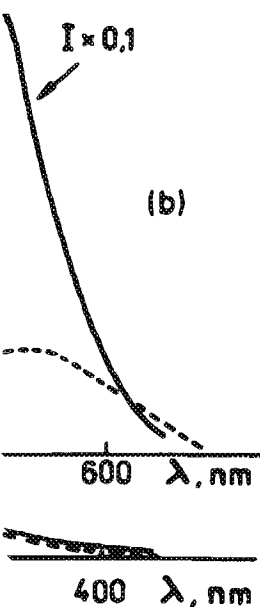


Figure 1(b) shows the absorption spectra of PNP upon binding to calf thymus DNA. The solid line represents the PNP-DNA complex, and the dashed line represents free PNP. The x-axis is wavelength λ in nm, with markers at 600 and 400 nm. The y-axis is labeled $I \times 0,1$. The solid line shows a red-shift and increase in intensity compared to the dashed line.

Figure 1(a) shows the difference spectra of PNP-DNA complexes. The x-axis is wavelength λ in nm, with markers at 330 and 300 nm. The y-axis is labeled $\Delta I \times 10^{-2}$. The solid line shows a red-shift and increase in intensity compared to the dashed line.

Figure 1(b) shows the fluorescence spectra of PNP upon binding to calf thymus DNA. The x-axis is wavelength λ in nm, with markers at 600 and 400 nm. The y-axis is labeled $I \times 0,1$. The solid line shows a red-shift and increase in intensity compared to the dashed line.

Figure 1(a) shows the difference spectra of PNP-DNA complexes. The x-axis is wavelength λ in nm, with markers at 330 and 300 nm. The y-axis is labeled $\Delta I \times 10^{-2}$. The solid line shows a red-shift and increase in intensity compared to the dashed line.

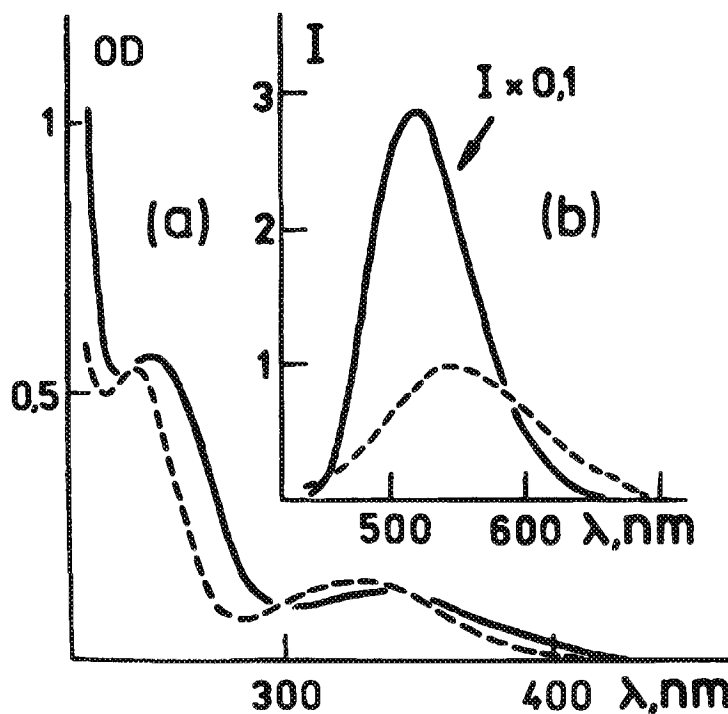


Figure 2: Changes observed in the absorption and fluorescence spectra of tridecapeptide upon binding to calf thymus DNA. (a) Absorption spectrum of free TDP (---) and difference absorption spectrum obtained by subtracting the spectrum of DNA from the spectrum of TDP-DNA complex (—). (b) Fluorescence spectra (uncorrected) of free TDP (---) and TDP in the presence of DNA (—). Concentration of TDP was $5 \cdot 10^{-5}$ M. DNA concentration was $1 \cdot 10^{-4}$ M (base pairs). Experimental conditions were identical to those in Figure 1.

200 nm with a slight shoulder near 220 nm. This indicates that a significant portion of the oligopeptide molecules is in a random-coiled conformation. On adding DNA to the oligopeptide solutions, the CD spectra are drastically changed. There is a great increase in the CD amplitude at about 195 nm. In addition, two negative CD bands appear at 213 and 255 nm. There is a remarkable similarity in the shapes of CD spectra obtained for DNA complexes with PNP, TDP and TVP (see refs. 1, 2, 5, 6). The fact that complexes with all the three peptides are characterized by a generally similar CD pattern argues that the peptides have common conformational features in the bound state. The β -structure is known to be the preferred conformation for N-protected oligo(L-valine)₇ in trifluoroethanol whereas oligo(L-valine)₃ assumes an unordered conformation (7). In aqueous solution, the equilibrium between β -associated species is shifted towards the formation of β -associated species (7). An increase in the amplitude of a positive CD band at 195 nm with a concomitant increase in the amplitude of a CD negative band near 220 nm seen after subtracting the DNA spectrum from the spectrum of the corresponding complex can be attributed to the formation of β -associated oligopeptide species upon binding to DNA. This is a reasonable suggestion since the ellipticities of free DNA are not large in the region 210-230 nm.

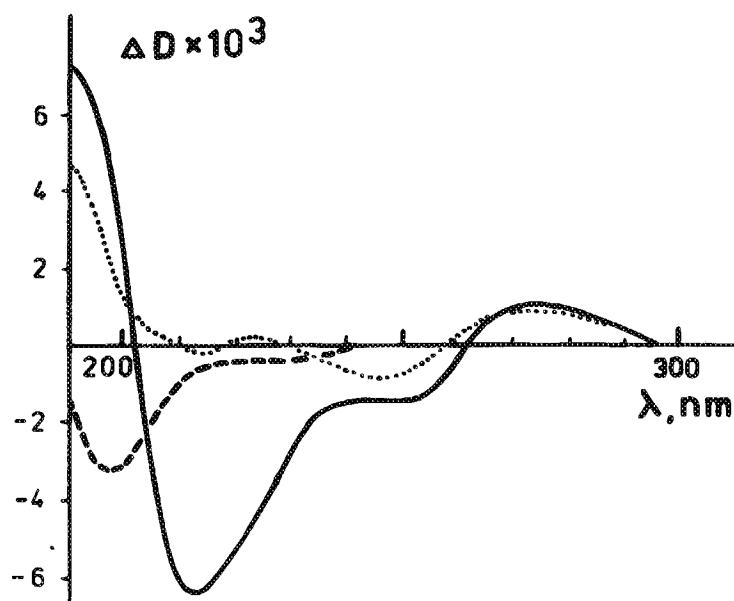


Figure 3: CD spectra of free PNP (---), PNP in the presence of calf thymus DNA (—) and of DNA alone (····). ΔD is the measured dichroism calculated per 1 cm pathlength cell. Concentration of PNP was $1 \cdot 10^{-4}$ M. DNA concentration was $1.25 \cdot 10^{-4}$ M (base pairs). Experimental conditions were identical to those in Figure 1.

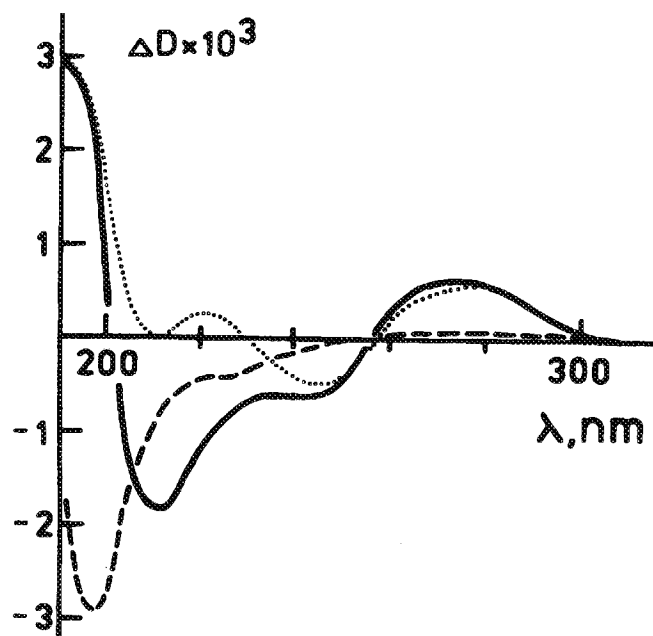
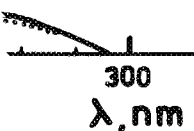
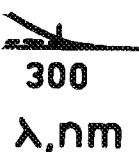


Figure 4: CD spectra of free TDP (---), TDP in the presence of calf thymus DNA (—) and of DNA alone (····). Concentration of TDP was $5 \cdot 10^{-5}$ M. DNA concentration was $1 \cdot 10^{-4}$ M. Experimental conditions were identical to those in Figure 1.



thymus DNA (—) and of DNA length cell. Concentration of PNP experimental conditions were identical



thymus DNA (—) and of DNA length cell. Concentration of PNP experimental conditions were identical

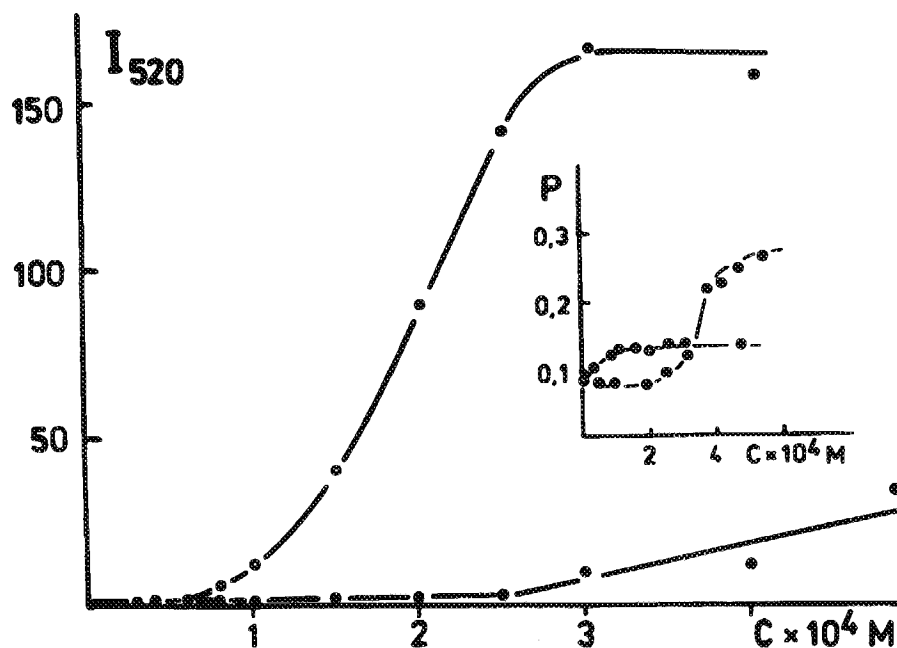


Figure 5: Plots of the fluorescence intensity measured at 520 nm against the peptide concentration for solutions of free PNP (1) and PNP in the presence of calf thymus DNA (2). Insert. Plots of the fluorescence polarization magnitude against concentration of PNP for solutions of free PNP (1) and PNP in the presence of DNA (2). DNA concentration was $3 \cdot 3 \cdot 10^{-5} \text{ M}$ (base pairs). Experimental conditions were identical to those in Figure 1.

In Figure 5 the intensity of fluorescence is plotted as a function of PNP concentration in the presence and absence of DNA in solution. The fluorescence intensities of PNP-DNA mixtures prepared at low peptide concentrations ($6 \cdot 10^{-5} \text{ M}$) are almost equal to the intensities measured for corresponding solutions of free oligopeptide. An increase in the peptide concentration within interval $1 \cdot 10^{-4} \text{ M} < c < 3 \cdot 10^{-4} \text{ M}$ results in a dramatic increase in the fluorescence intensity. Presumably, DNA binds a significant amount of the oligopeptide in a cooperative manner. The fluorescence intensity of pentapeptide-DNA mixture prepared at high input peptide/DNA ratios ($2 C/P > 2$) exceeds the fluorescence intensity of the free oligopeptide by approximately two orders of magnitude. The contribution of bound monomers to the fluorescence intensity of complexes obtained at high $2 C/P$ values can be neglected.

Figure 5 (insert) displays the plots of the fluorescence polarization versus peptide concentrations for solutions containing free PNP and PNP-DNA mixtures. As seen in Figure 5, the magnitude of the fluorescence polarization is equal to about 0.06, if the free peptide concentration does not exceed $2 \cdot 10^{-4} \text{ M}$. It is noteworthy that the fluorescence polarization measured for pentapeptide-DNA mixtures under the same conditions exceeds approximately two-fold the value found for the oligopeptide in free solution. This occurs at very low $2 C/P$ values when changes in the fluorescence intensity on adding DNA to an oligopeptide solution are negligible. We interpret these observations as indicating that there exist at least two kinds of bound pentapeptide forms.

The first one, occurring predominantly at low $2C/P$ values ($2C/P < 0.1$), has almost the same fluorescence intensity per mole of peptide and the same molar extinction coefficient at 330 nm as those found in free peptide solutions. As seen in Figure 5, an increase in the peptide concentration within the limits $2 \cdot 10^{-4} \text{M} < C < 5 \cdot 10^{-4} \text{M}$ results in a dramatic increase in the magnitude of the fluorescence polarization which reflects the formation of massive aggregates in free solution. These aggregates can be visualized by electron microscopy (6).

Sequence Specificity of Binding Processes

Fluorescence measurements provide a rather simple and sensitive tool for comparing the affinities of the pentapeptide to various DNAs and synthetic polynucleotides. Figure 6 shows the plots of the fluorescence intensity at 520 nm against nucleic acid concentration for titration of PNP with poly(dG) · poly(dC), poly[d(A-C)] · poly[d(G-T)] and poly(dA) · poly(dT). It can be seen that the fluorescence intensity at relatively high nucleic acid/peptide ratios decreases in the following order: poly(dG) · poly(dC) > poly[d(A-C)] · poly[d(G-T)] > poly(dA) · poly(dT), thereby suggesting the same order of sequence preferences for binding of β -associated species of PNP to DNA. A similar series of experiments has been also performed for binding of TVP and TDP to various natural and synthetic DNAs (data not shown). These two oligopeptides in self-associated forms also bind to DNA in a sequence-specific manner. It has been found that TVP binds more strongly to poly(dG) · poly(dC) than to poly(dA) · poly(dT) (1,8). This is confirmed by fluorescence and equilibrium dialysis measurements using three-part dialysis cells similar to those described by Muller and Grothers (9). From the experimental curves obtained from binding of TDP to various nucleic acids, a conclusion can be drawn that this oligopeptide exhibits a quite distinct order of sequence preferences as compared with that of TVP or PNP (Figure 7). It binds more strongly to poly[d(A-C)] · poly[d(G-T)] and poly(dA) · poly(dT) than to poly(dG) · poly(dC). The affinity order observed for the binding of PNP to various synthetic DNAs is confirmed by experiments in which the effect of added sodium ions on the stabilities of peptide-DNA complexes is studied. From Figure 6 one can see that complexes of PNP with poly(dA) · poly(dT) are completely destroyed in the presence of 0.05 M NaCl whereas complexes with poly(dG) · poly(dC) are stable even in the presence of 0.2 M NaCl.

Electron Microscopy Studies of Peptide-DNA Complexes

The morphology of DNA complexes with TDP and PNP was studied by electron microscopy at different input peptide/DNA ratios. Micrographs for complexes with the same DNA concentration of TDP and PNP are shown in Figures 8, 9, and 10, respectively. The comparison of micrographs corresponding to different stages of the DNA compaction upon interaction with TDP and PNP clearly shows that the main features of the DNA condensation in both cases are similar.

It should be noted that in the absence of the peptide or at very low peptide concentrations ($C < 10^{-6} \text{M}$) the DNA is poorly absorbed on electron microscopic support films. The DNA fibers on such preparations are stretched and tend to form separate clusters.

s ($2C/P < 0.1$), has almost the same molar extinction coefficients. As seen in Figure 5, an $10^{-4}M < C < 5 \cdot 10^{-4}M$ fluorescence polarization resolution. These aggregates

sensitive tool for comparing synthetic polynucleotides. 10 nm against poly(dA-C) · poly(dG-T) fluorescence intensity at relatively low order: poly(dG) · poly(dC) > poly(dA) · poly(dT) thereby suggesting the same species of PNP to DNA. A binding of TVP and TDP to these two oligopeptides in a specific manner. It has been shown that poly(dA) · poly(dT) is more stable than poly(dA) · poly(dT) in dialysis measurements by Muller and Grothers (9). TDP to various nucleic acids exhibits a quite distinct binding of PNP to various synthetic polynucleotides. The effect of added sodium chloride completely destroyed in the poly(dG) · poly(dC) are stable

was studied by electron micrographs for complexes with DNA in Figures 8, 9, and 10, leading to different stages of PNP clearly shows that the complexes are similar.

low peptide concentrations on microscopic support films. The complexes form separate clusters.

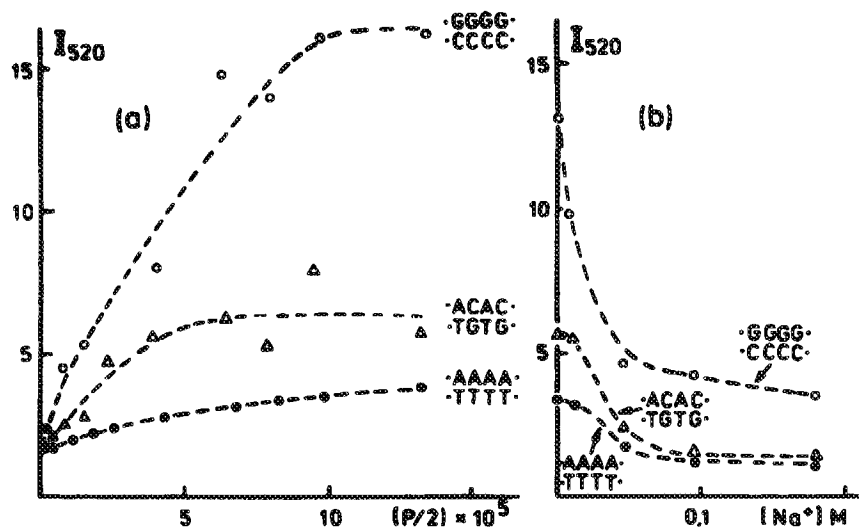


Figure 6: (a) The fluorescence intensity at 520 nm plotted against nucleic acid concentration (P/2) for titration of PNP solution with poly(dG) · poly(dC) (○), poly[d(A-C)] · poly[d(G-T)] (Δ) and poly(dA) · poly(dT) (●). Concentration of PNP was $5 \cdot 10^{-5}M$. Experimental conditions were identical to those in Figure 1. (b) The effect of added NaCl on the stability of complexes formed by PNP with poly(dG) · poly(dC) (○), poly[d(A-C)] · poly[d(G-T)] (Δ) and poly(dA) · poly(dT) (●). The fluorescence intensity of peptide-DNA mixtures at 520 nm is plotted versus molar concentration of NaCl.

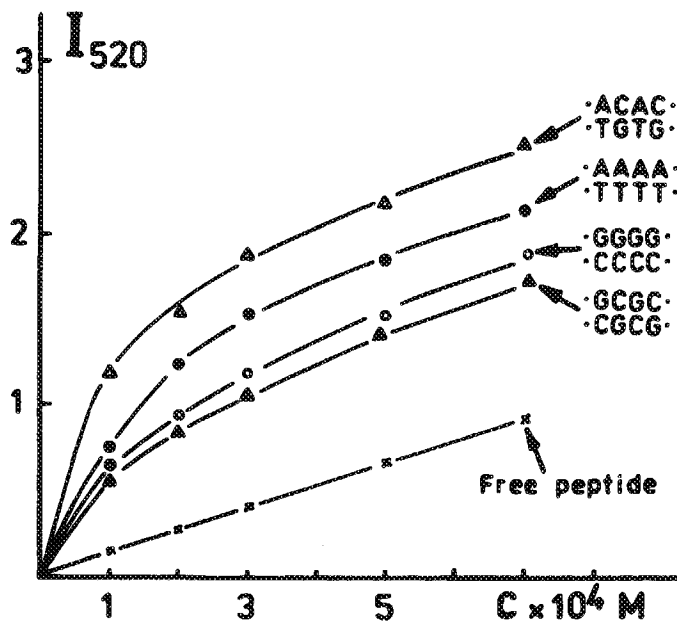


Figure 7: Titration of various synthetic polynucleotides with TDP. DNA concentration in the titration assay was $1.6 \cdot 10^{-6}M$ (base pairs). I_{520} is the fluorescence intensity of TDP measured at 520 nm and excited at 380 nm. C is the molar concentration of TDP. The titration curves were measured at $20^\circ C$ in 1 mM Na-cacodylate buffer (pH 7.0) in the presence of $5 \cdot 10^{-4}M$ $MgCl_2$ and 25% (v/v) methanol.

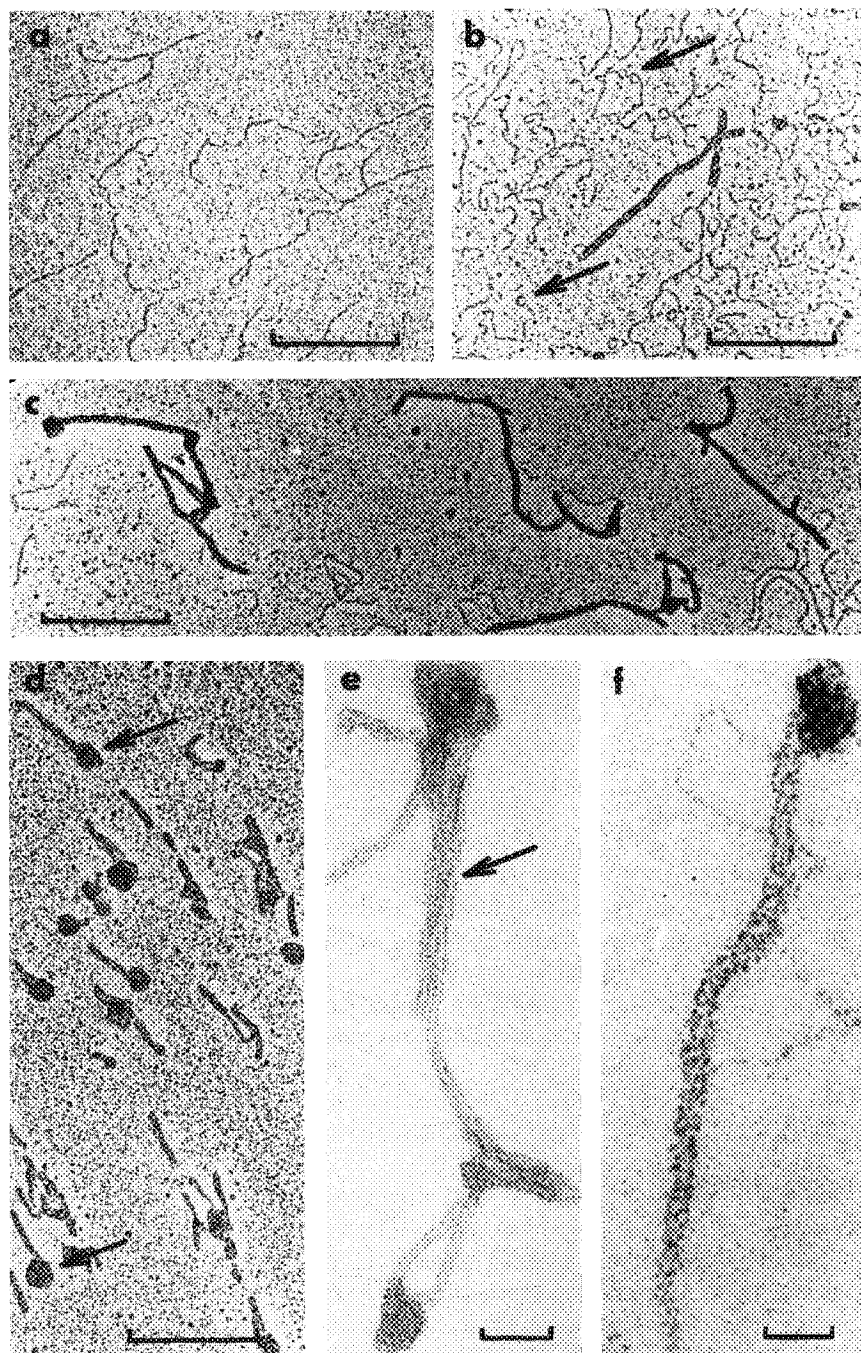
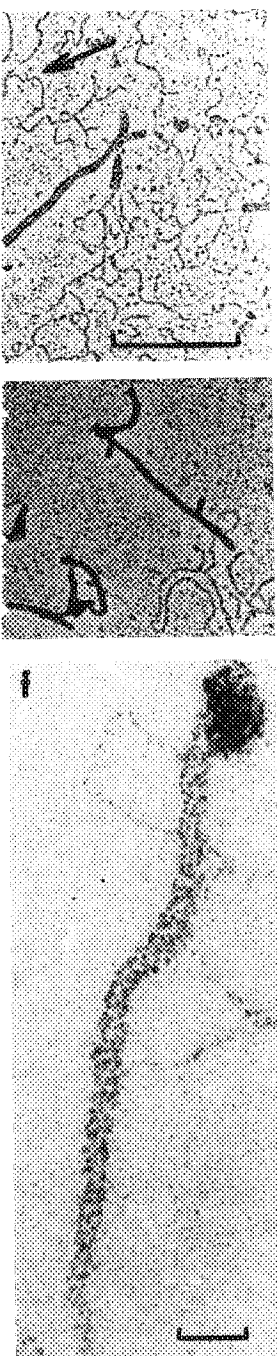


Figure 8: Electron micrographs of thymus DNA complexes with TDP at various TDP concentrations. DNA concentration in all preparations was $1.6 \cdot 10^{-3}$ M (base pairs). Concentrations of TDP were $1 \cdot 10^{-6}$ M (a); $3 \cdot 10^{-6}$ M (b); $5 \cdot 10^{-6}$ M (c); $1.5 \cdot 10^{-5}$ M (d-f). Contrasting by rotary shadowing (a-d) and uranyl acetate staining (e and f). The bars represent 300 nm (a-d) and 40 nm (e and f).



DNA complexes with TDP at various TDP concentrations. (a-d) Contrasting by rotary shadowing (a-d) and uranyl acetate staining (e and f). The bars represent 300 nm (a) and 40 nm (e and f).

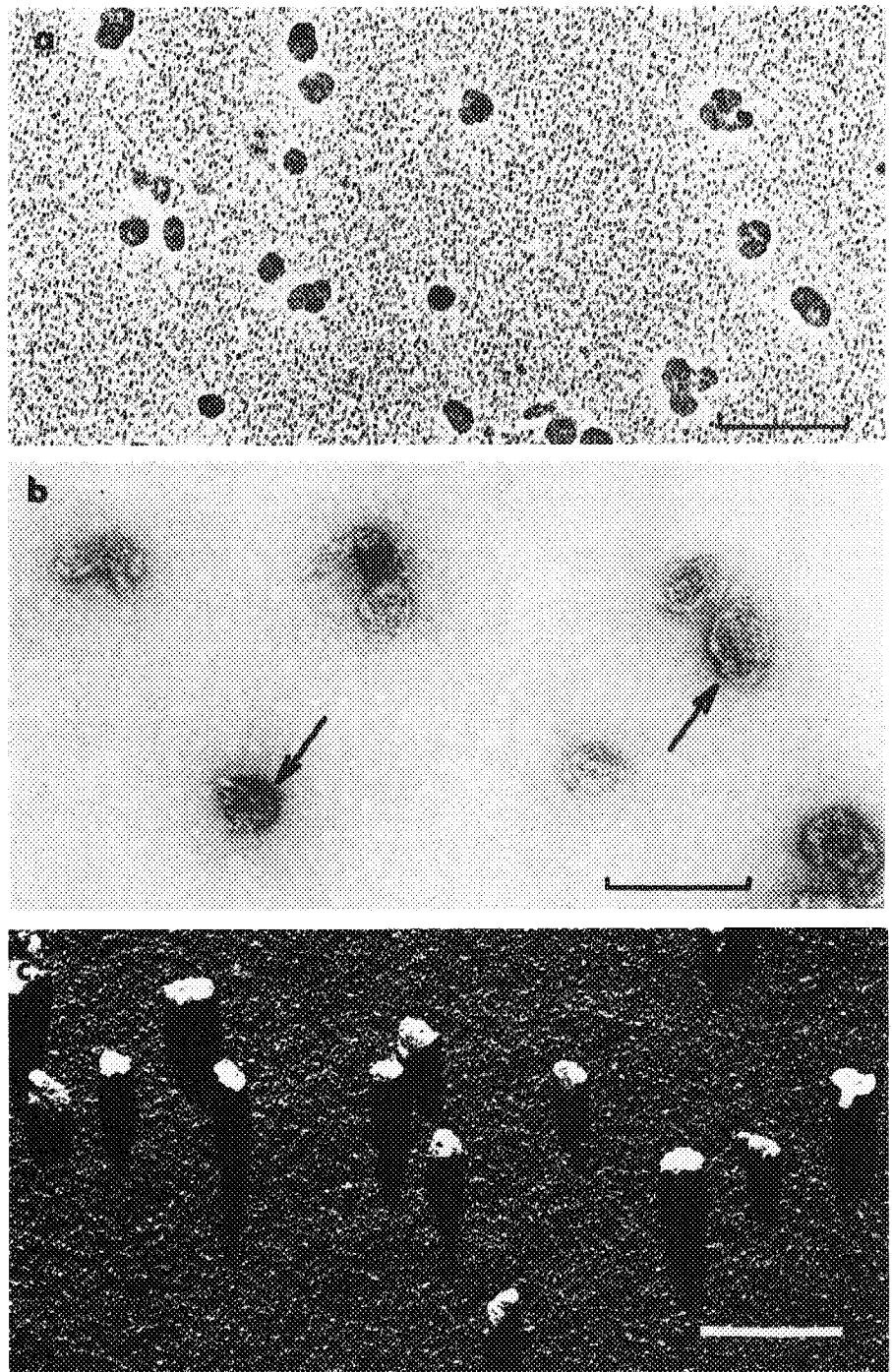


Figure 9: Electron micrographs of thymus DNA complexes with TDP at the peptide concentration of about $5 \cdot 10^{-5} M$ (the globular particles). Contrasting by rotary shadowing (a), uranyl acetate staining (b) and shadowing from a fixed direction (c). The bars represent 300 nm, (a), 80 nm (b) and 250 nm (c).

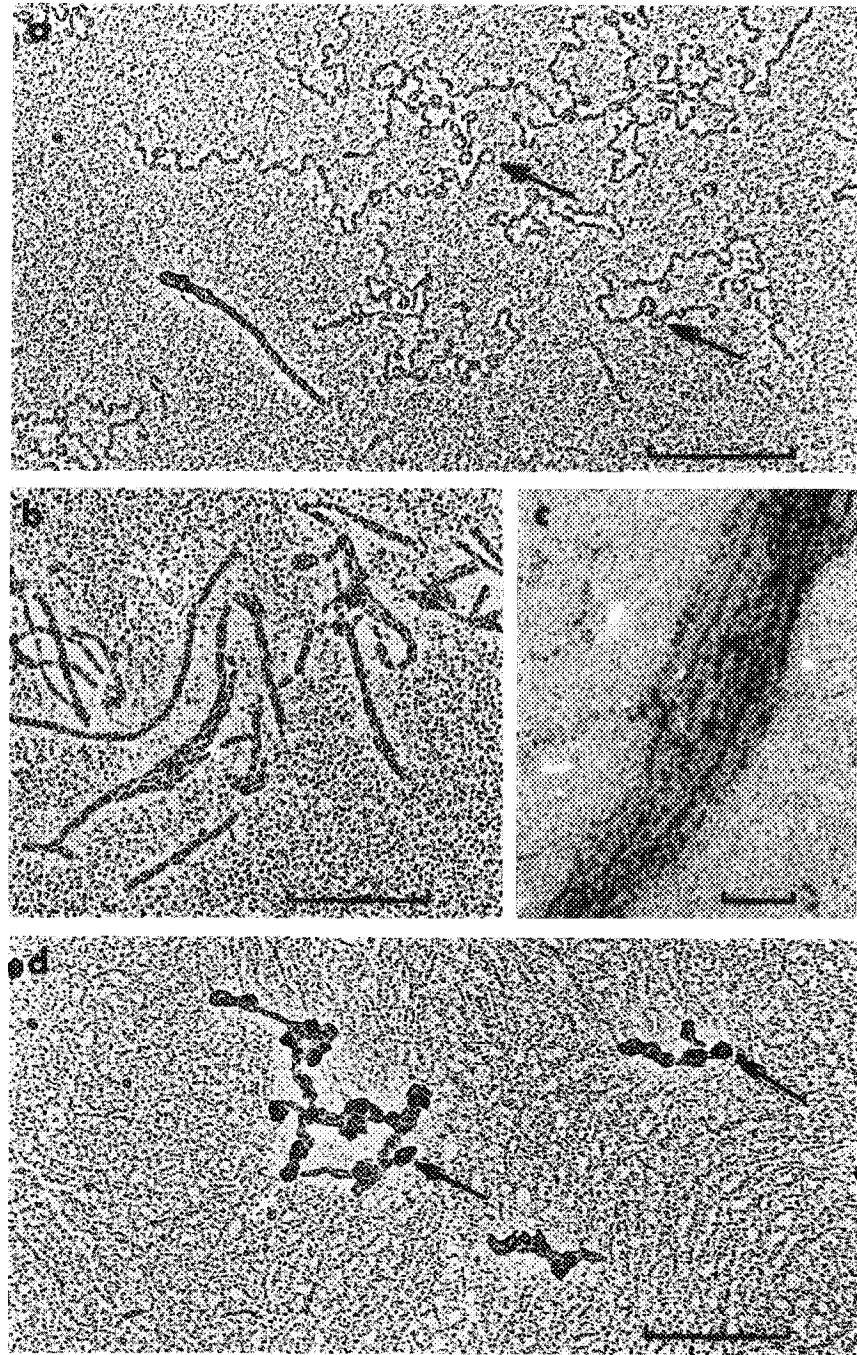


Figure 10: Electron micrographs of linear DNA complexes with PNP at various peptide concentrations. DNA concentration in all these preparations was about $1.6 \cdot 10^{-5}$ M (base pairs). Concentrations of PNP were $3 \cdot 10^{-5}$ M (a); $7 \cdot 10^{-5}$ M (b and c); $1.5 \cdot 10^{-4}$ M (d). Contrasting by rotary shadowing (a, b and d) and uranyl acetate staining (c). The bars represent 400 nm (a, b and d) and 20 nm (c).



Figure 8a shows a micrograph of DNA in the presence of 10^{-6} M TDP. It can be seen that extended 40-60 Å thick fibers predominate. These fibers are typical in morphology of free DNA prepared by direct absorption on support films. DNA-PNP complexes at the same peptide concentrations have the same appearance.

In Figures 8b and 10a micrographs of DNA-TDP and DNA-PNP complexes (input peptide concentrations of $2.5 \cdot 10^{-6}$ M and $3.5 \cdot 10^{-5}$ M) are shown, respectively. It can be seen that an increase in the peptide concentration improves the DNA absorption on support films. In both preparations the major part of the material is represented by 40-60 Å thick fibers having "curly" appearance. Such fibers often have regions where DNA makes nearly a complete turn, forming a small loop. These loops may be completely closed or not. They occur in the middle part of a fiber or at its ends. Most of the loops are about 200 Å in diameter. Several loops are indicated in Figure 8b and Figure 10a by arrows.

Besides the above described "curly" fibers, dense rod-shaped structures are observed on the same preparations. These structures are about 200 Å thick on preparations contrasted by rotary shadowing. Their morphology resembles rod-shaped structures observed in complexes of linear DNA with TVP (3). When the peptide concentration is increased up to $5 \cdot 10^{-6}$ M, rod-like compact structures begin to prevail (Figures 8c and 10b). In the immediate contact with compact structures, noncondensed 40-60 Å thick fibers are often observed (Figure 8c). Complexes of DNA with PNP at the same 2 C/P values have similar appearances, though in the case of PNP the material has a more pronounced tendency to form aggregates.

At higher input TDP concentrations the morphology of TDP-DNA complexes looks different (Figure 8d). 40-60 Å fibers are practically absent. The major part of the material is represented by compact rods. Many of them have a globule at one of the ends (shown by arrows in Figure 8d). The sizes of the globular parts in such "comma-shaped" particles vary considerably. The analysis of many "comma-shaped" particles in different preparations shows that when the TDP concentration is raised the globular part has a tendency to become greater at the expense of the length of the fibrillar particles. A "comma-shaped" particle containing both globular and fibrillar parts will be further referred to as an intermediate structure.

High-magnification micrographs of intermediate structures after staining with uranyl acetate are shown in Figure 8e and 8f. It can be seen that these structures have the same morphology as on shadowed preparations. The thickness of compact fibers in uranyl acetate stained preparations is 80-100 Å. It should be noted that uranyl acetate staining causes aggregation of DNA-peptide complexes, but even in the aggregated state, compact rod-like regions preserve their structural integrity (arrow in Figure 8e).

The appearance of DNA-PNP complexes corresponding to the condensation step is shown in Figure 10b and 10c. As has been already noted, DNA-PNP complexes look much more aggregated, though in their general morphology the observed rods are similar to the compact rods, observed for DNA-TDP complexes. Figure 10c shows a high-magnification photograph of a portion of an aggregate of compact rods observed

in DNA-PNP complexes. It is evident that this aggregate is formed by lying side-by-side 100 Å compact fibers.

At input TDP and PNP concentrations over $5 \cdot 10^{-5}$ M and $1.4 \cdot 10^{-4}$ M, respectively, practically all the material on electron microscopic preparations is presented by dense globules (Figures 9 and 10d). The globular particles of DNA-TDP complexes in most cases lie well apart from each other. The compact globules of DNA-PNP complexes form large aggregates on the preparations, but even in these aggregates individual particles do not lose their characteristic shape and organization (arrows in Figure 10d).

Micrographs of uranyl acetate stained DNA-TDP complexes at high TDP concentrations are shown in Figure 9b. Most of the dense particles retain their structure after uranyl acetate staining. In the structure of some particles, segments of 100 Å fibers can be seen (arrows in Figure 9b). The analysis of intermediate structures with long and short tails and of compact globules on shadowed and stained preparations suggests that globular particles are built of tightly wrapped 100 Å fibers, structurally identical to those present in compact rods.

Most of the globules contrasted with uranyl acetate have a diameter of 300-400 Å. Taking into account the average length of initial calf thymus DNA molecules (about 5000 base pairs), it can be assumed that each globule contains a single DNA molecule, i.e., the compaction has an intramolecular character. Variations in the globule sizes can be ascribed to the heterogeneity of calf thymus DNA preparations.

In order to obtain a more reliable information concerning the nature of the compaction process, additional experiments were carried out with linear DNA of a fixed molecular length (linearized pBR 322 DNA). In general, compaction of linearized pBR 322 DNA proceeds in the same way as that of calf thymus DNA. At high peptide concentrations, dense globular particles were mainly observed on the preparations. Since uranyl acetate can cause disruption of compact globules, thereby artificially increasing the heterogeneity of the material, the diameters of compact globules in pBR 322 DNA complexes with TDP and PNP were measured on shadowed preparations.

The results of these measurements are shown in Figures 11 and 12, respectively. It can be seen that the histogram for DNA-TDP complexes has only one peak and the particle diameters vary insignificantly. It can be concluded that all the particles in such preparations contain equal numbers of DNA molecules. Rough estimations of the particle volumes, if they are considered to have a spherical shape, show that dense globules can contain either one or two pBR 322 DNA molecules.

In order to draw a more definite conclusion, additional information about the height of the particles is required. The height of the particles can be measured on electron microscopic preparations shadowed at a known angle in one direction (Figure 9c). The results of such measurements show that globules are disc-shaped rather than spherical and their heights are equal roughly to one half of their diameters.

is formed by lying side-by-

nd $1.4 \cdot 10^{-4}$ M, respectively, preparations is presented by es of DNA-TDP complexes pact globules of DNA-PNP out even in these aggregates be and organization (arrows

plexes at high TDP concen- rticles retain their structure particles, segments of 100 Å intermediate structures with ed and stained preparations ped 100 Å fibers, structurally

ave a diameter of 300-400 Å. ymus DNA molecules (about ule contains a single DNA character. Variations in the thymus DNA preparations.

g the nature of the compaction ear DNA of a fixed molecular ction of linearized pBR 322 NA. At high peptide concen- d on the preparations. Since thereby artificially increasing compact globules in pBR 322 on shadowed preparations.

res 11 and 12, respectively. It es has only one peak and the luded that all the particles in ecules. Rough estimations of a spherical shape, show that 2 DNA molecules.

ional information about the particles can be measured on own angle in one direction hat globules are disc-shaped roughly to one half of their

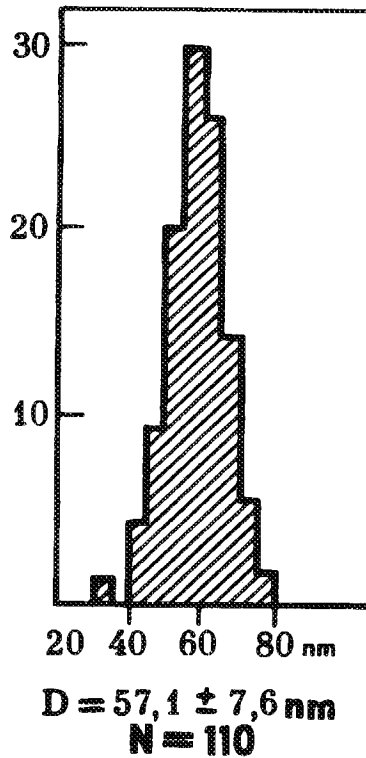


Figure 11: Histogram of the globular particles diameters obtained for complexes of TDP with a linearized plasmid pBR 322.

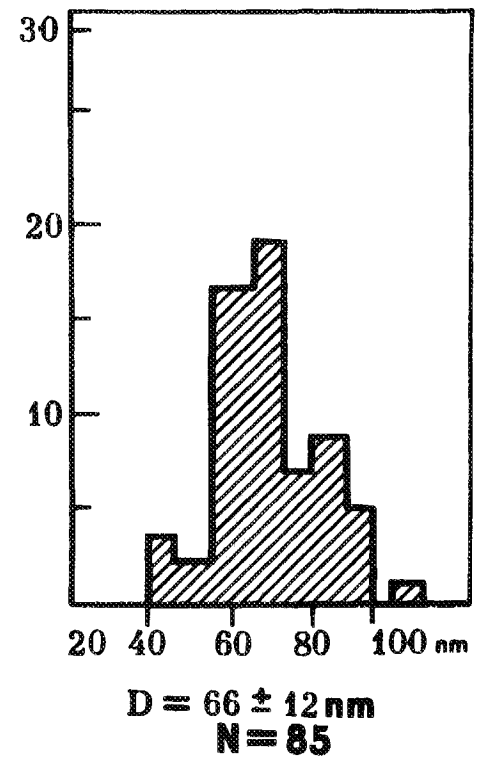


Figure 12: Histogram of the globular particles diameters obtained for complexes of PNP with a linearized plasmid pBR 322.

These results coupled with other data enable one to estimate the volume of dense particles in DNA-TDP complexes, which is equal to $1.3 \cdot 10^7 \text{ \AA}^3$. If we further assume that in dense compact globular structures the DNA is packed with the same density as in dense compact toroidal structures (10), the volume of each particle corresponds to the molecular volume of DNA.

The histogram in Figure 12 shows the results of the same measurements for compact globules observed in pBR 322 DNA-PNP complexes. In this case, particles lying apart from the aggregates were measured. It should be noted that particles forming aggregates were of the same size, but they were not included in the histogram. It can be seen in the histogram that the variation in the diameters of globules is rather small but exceeds that found for DNA-TDP complexes.

The diameter of globules corresponding to the most frequently met size of globules obtained with PNP is nearly the same as for globules observed in the case of pBR 322 DNA-TDP complexes.

It should be noted that in preparations of DNA-PNP complexes a number of globules with larger diameters are present. However, a relative fraction of these

globules is small and the peak that corresponds to them on the histogram is clearly minor (Figure 12). Probably, these globules contain two DNA molecules. It is also possible that large globules are aggregates of smaller globules.

In general, our results show that most of dense globules observed at high PNP/DNA ratios also contain only one DNA molecule. It can be concluded that the condensation of DNA upon interaction with TDP and PNP has the same general features and leads to the formation of compact particles, each containing only one DNA molecule.

Discussion

Concentration dependence of spectroscopic data obtained for PNP and TDP indicates that these two peptides can self-associate in aqueous solutions forming aggregates of varying sizes that are in concentration-dependent equilibria with each other and with monomers.

General shapes of the experimental curves obtained from DNA titration with PNP and TDP strongly suggest that these two peptides bind to DNA both in the monomeric and self-associated forms. However, the binding affinities of the two peptides for DNA are low at a concentration level of free peptide of about $1 \cdot 10^{-6}$ M when these two peptides exist predominantly in the monomeric forms. The DNA-binding activity of PNP (or TDP) greatly increases when self-associated peptide species are present in solution, as follows from the existence of concentration-dependent changes in the shapes of absorption and fluorescence spectra. We conclude that self-associated peptide species have a greater affinity for DNA than monomers.

From literature data it is well known that β -strands are often organized into complex assemblies that take the form of sheets and sandwiches (11,12). The appearance of CD bands induced upon binding of PNP and TDP to DNA indicates that the two peptides assume an ordered conformation in peptide-DNA complexes. In contrast, CD patterns of PNP and TDP in free solutions are characteristic of a random coiled conformation. The difference CD spectra obtained by subtracting the spectra of free DNA from the spectra of PNP-DNA complexes have β -structure-like shapes with positive and negative CD bands at 196 nm and 220 nm, respectively. The difference CD spectrum which can be calculated from the spectra of TDP-DNA complexes (see Figure 4) also has a negative CD band near 215 nm, whereas a positive CD band at 195 is absent. This reflects the fact that in TDP-DNA mixtures a significant part of the peptide molecules are unbound and exist in a random coiled conformation. In this case, the difference CD spectrum can be represented as a sum of the CD spectrum of bound peptide in the β -conformation and the spectrum of free peptide with a negative CD band at 197 nm.

Previous studies have shown that TVP and TDP bind in the minor DNA groove because they bind in a sequence-specific manner to glucosylated DNA whose major groove is filled in with bulky glucose and diglucose residues (1). In addition, an antibiotic distamycin which binds in the minor DNA groove at AT-rich regions can displace these peptide molecules from their complexes with DNA (1, 6, 8). Previous

on the histogram is clearly two DNA molecules. It is also globules.

observed at high PNP/DNA included that the condensation the same general features and naming only one DNA molecule.

obtained for PNP and TDP in aqueous solutions forming dependent equilibria with each

from DNA titration with PNP to DNA both in the monomeric nities of the two peptides for of about $1 \cdot 10^{-6}M$ when these ic forms. The DNA-binding associated peptide species are of concentration-dependent ce spectra. We conclude that y for DNA than monomers.

often organized into complex es (11,12). The appearance of to DNA indicates that the two -DNA complexes. In contrast, aracteristic of a random coiled y subtracting the spectra of free e β -structure-like shapes with n, respectively. The difference tra of TDP-DNA complexes n, whereas a positive CD band A mixtures a significant part of ndom coiled conformation. In nted as a sum of the CD spec- e spectrum of free peptide with

nd in the minor DNA groove to glucosylated DNA whose ucoside residues (1). In addition, DNA groove at AT-rich regions exes with DNA (1, 6, 8). Previous

observations have also shown that TVP and TDP in the β -associated form exhibit preferences for certain base pair DNA sequences (1, 2, 5). Our present observations coupled with other data (1,13) indicate that there are differences in the affinity order displayed by each oligopeptide for various DNA base pair sequences. TVP and PNP in the β -associated forms bind more strongly to poly(dG) · poly(dC) than to poly(dA) · poly(dT), whereas TDP exhibits an opposite order of sequence preferences binding more strongly to poly[d(A-C)] · poly[d(G-T)] and poly(dA) · poly(dT) than to poly(dG) · poly(dC). These binding preferences are consistent with the recognition code proposed earlier for the description of sequence-specific interactions between β -structure forming peptides and DNA (14-16).

Since valyl side chains are inert, the observed preference of TVP for binding to poly(dG) · poly(dC) is probably attributed to hydrogen bonding interactions between the backbone NH and CO groups in dimeric TVP species and GC pairs. This is in agreement with the stereochemical model proposed for binding to DNA of regulatory proteins containing antiparallel β -strands in their DNA-binding domains (14,16). According to the model, the backbone NH and CO groups of the two antiparallel peptide chains are hydrogen bonded to the functional groups of DNA base pairs exposed in the minor groove. This recognition mechanism is realized on binding of an oligopeptide antibiotic triostin A to DNA as follows from the three-dimensional structure of a complex between triostin A and oligonucleotide 5'-GCATGC-3' (17). We believe that β -associated species of TVP, PNP, and TDP bind to DNA in almost the same manner as do the antiparallel peptide chains in the crystalline triostin A-DNA complex.

The binding of PNP and TDP is a cooperative phenomenon. The sequence-specific binding of β -associated peptide species to DNA is evidently accompanied by the cooperative process of condensation of peptide molecules in the minor DNA groove and formation of β -sandwiches (1,13). In a bound β -sandwich the two peptide dimers occupy nonequivalent spatial positions. One of them establish specific contacts with DNA base pairs on the floor of the minor groove, whereas the other lies above the first one and can interact with the sugar-phosphate backbone of DNA. This model implies that at high levels of occupancy a part of bound peptide molecules are exposed on the outer surface of DNA and are accessible for the interaction with other bound peptide molecules. Perhaps, these interactions are responsible for side-by-side association of DNA segments in compact rod-like structures observed by electron microscopy. Examination of electron micrographs for complexes of DNA with TVP, PNP, and TDP shows that compact rod-like structures in all these complexes are basically similar in their morphology. Electron microscopy studies also show that TDP and PNP cause intramolecular condensation of linear DNA with the formation of globular particles. The formation of globules is also observed in TVP-DNA complexes (data not shown).

It seems possible to propose a general model describing the formation of compact particles in complexes of DNA with any of the three peptides. The two schematic drawings presented in Figures 13 and 14 illustrate the main steps of the compaction process as well as the proposed arrangement of DNA fibers in the compact structures

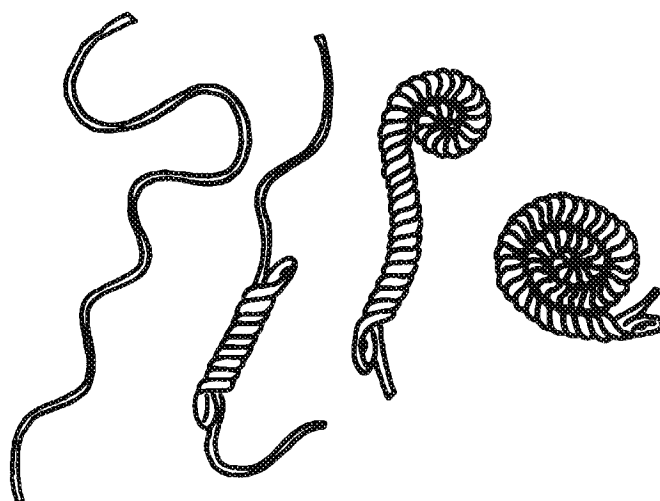


Figure 13: A scheme illustrating the main steps of the compaction process of linear DNA stimulated by the interaction with TDP or PNP.

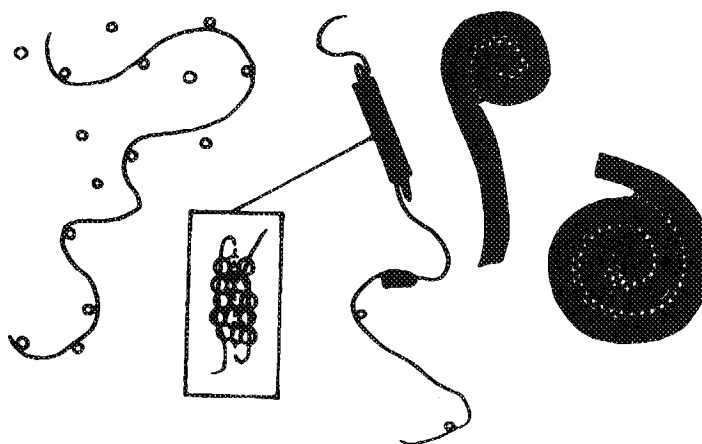


Figure 14: A hypothetical scheme of spatial organization of DNA-peptide complexes. Interaction between peptide molecules bound to various DNA segments is responsible for side-by-side arrangement and coalescence of DNA segments which leads to the formation of a characteristic three-dimensional structure of DNA. In the rod-like compact structures observed by electron microscopy, peptide molecules probably form internal "core" over which DNA is wound. Peptide molecules are shown by circles.

and probable arrangement of bound peptide molecules on DNA. It is assumed that interaction between bound peptide molecules stimulates side-by-side association of DNA segments.

At the initial stages of condensation at low peptide/DNA ratios ($2C/P < 1$), the peptide molecules cause the formation of small DNA loops either due to a change in the DNA persistent length or due to a local DNA bending. At higher peptide/DNA ratios, hydrophobic interactions between bound peptide molecules or their clusters

on DNA cause side-by-side association of DNA segments and thus the first compact regions are formed.

To our regret, it is impossible to draw definite conclusions concerning the organization of DNA in compact regions on the basis of the results obtained with linear DNA. A thorough analysis of the structure of compact regions in TDP and PNP/DNA complexes shows that they are formed by several duplex DNA segments lying side-by-side, although the exact number of these segments cannot be determined.

The most reliable information about DNA arrangement in the compact rod-like regions has been obtained for complexes of TVP with circular supercoiled DNA (4). In this case, it has been shown that compact regions contain interwound double-stranded DNA segments lying side-by-side. Since all the peptides under study belong to a class of β -structure forming peptides and exhibit similar DNA binding properties, it seems probable that compact rods in complexes of PNP and TDP with linear DNA have the same organization as compact regions of triple rings observed in complexes of TVP with circular supercoiled DNA (4). This is schematically shown in Figures 13 and 14. However, it should be noted that further studies are needed to determine the exact number of double-stranded DNA segments in the compact regions. Bound peptide molecules are probably located mainly inside the compact structure whereas the DNA regions not occupied by peptide molecules are exposed on the outer surface of the structure. If we take into account the inherent capacity of three peptides to self-associate in aqueous solutions, the structure where peptide molecules are hidden in the "core" of compact rods and the hydrophilic DNA is exposed to the solvent, seems to be plausible. The insert in Figure 14 demonstrates this feature of the structure though in this drawing three DNA fibers are shown without interwinding in order to simplify the picture.

Our observations show that compaction process accompanying the binding of PNP (or TDP) to DNA is of intramolecular nature. It should be mentioned that DNA condensation induced by peptide binding can be either intramolecular process (formation of compact rings upon binding of TVP to a supercoiled DNA or formation of compact globules in the complexes with PNP and TDP) or intermolecular one (formation of toroids in the complexes with TVP (18)).

In our opinion, the fate of compaction process and discrimination between intra- or intermolecular type of resulting structures is determined at the early stages of the compaction process. A key factor is the formation at the initial stages of condensation of a nucleus of corresponding compact structure where most of the peptide binding sites on DNA are occupied and engaged in the appropriate interactions. Whenever a stable nucleus is formed, further growth of the compact region can be much more probable with the involvement of noncondensed parts of the same molecule rather than of DNA segments belonging to other molecules. In this case mono-molecular condensation takes place.

A necessary condition for the intracellular condensation is the absence of "stickiness" of compact regions or compact structures at the initial stages of compaction with

process of linear DNA stimulated by

peptide complexes. Interaction between
ble for side-by-side arrangement and
characteristic three-dimensional structure of
microscopy, peptide molecules probably
cles are shown by circles.

cles on DNA. It is assumed that
ulates side-by-side association

NA ratios ($2C/P < 1$), the peptide
s either due to a change in the
nding. At higher peptide/DNA
ptide molecules or their clusters

respect to the non-compacted DNA. It is likely that compact rod-like structures observed in the complexes of TDP and PNP with DNA as well as triple regions in the complexes of TVP with circular supercoiled DNA satisfy this requirement. This viewpoint is confirmed by the fact that the association of the above mentioned ordered compact structures with decondensed DNA is observed rather rarely in electron microscopic preparations. Rod-like structures in TDP-DNA complexes retain their structural integrity in aggregates and self-associate with the formation of globules only at very high peptide/DNA ratios. The situation is different when intermolecular compaction takes place. An example is a toroidal structure arising on binding of circular relaxed DNA to TVP. Here at the intermediate stages of the DNA condensation, one can observe non-compacted DNA molecules absorbing on toroids (18).

The data presented here demonstrate that complexes of synthetic peptides with DNA can serve as suitable model systems for the studies of DNA compaction. Electron microscopic studies of complexes of linear DNA and circular supercoiled DNA with β -structure forming peptides have led to the discovery of a spectrum of various compact structures corresponding to different levels of DNA compaction.

Reference and Footnotes

1. G.V. Gursky, A.S. Zasedatelev, A.L. Zhuze, A.A. Khorlin, S.L. Grokhovsky, S.A. Streltsov, A.N. Surovaya, S.M. Nikitin, A.S. Krylov, V.O. Retchinsky, M.V. Mikhailov, R.S. Beabealashvili and B.P. Gottikh, *Cold Spring Harbor Symp. Quant. Biol.* 47, 367 (1983).
2. S.A. Streltsov, A.A. Khorlin, A.N. Surovaya, G.V. Gursky, A.S. Zasedatelev, A.L. Zhuze and B.P. Gottikh, *Biofizika (USSR)* 25, 929 (1980).
3. V.L. Makarov, S.A. Streltsov, Y.Y. Vengerov, A.A. Khorlin and G.V. Gursky, *Molekul. Biol. (USSR)* 17, 1089 (1983).
4. Y.Y. Vengerov, T.E. Semenov, S.A. Streltsov, V.L. Makarov, A.A. Khorlin, G.V. Gursky, *J. Mol. Biol.* 184, 251 (1985).
5. T.E. Semenov, Y.Y. Vengerov, A.N. Surovaya, N.Yu. Sidorova, S.A. Streltsov, A.A. Khorlin, A.L. Zhuze, B.P. Gottikh and G.V. Gursky, *Molekul. Biol. (USSR)* 20, 1422 (1986).
6. N.Yu. Sidorova, T.E. Semenov, A.N. Surovaya, Y.Y. Vengerov, S.A. Streltsov, A.A. Khorlin, B.P. Gottikh, A.L. Zhuze and G.V. Gursky, *Molekul. Biol. (USSR)* 21, 1534 (1987).
7. C. Toniolo and G.M. Bonora, *Macromol. Chem.* 175, 2203 (1974).
8. S.A. Streltsov, A.A. Khorlin, A.N. Surovaya, G.V. Gursky, A.S. Zasedatelev, Yu.D. Nechipurenko, A.L. Zhuze and B.P. Gottikh, *Studia Biophysica* 87, 189 (1982).
9. W. Muller and D.M. Grothers, *Eur. J. Biochem.* 54, 267 (1975).
10. W.C. Earnshaw and S.R. Casjens, *Cell* 21, 319 (1980).
11. K.-C. Chon, G. Nemethy, S. Rumsey, R.W. Tuttle and H.A. Scheraga, *J. Mol. Biol.* 186, 641 (1986).
12. C. Chothia and J. Janin, *Proc. Natl. Acad. Sci. USA* 78, 4146 (1981).
13. T.A. Leinsoo, V.A. Nikolaev, S.L. Grokhovsky, S.A. Streltsov, A.S. Zasedatelev, A.L. Zhuze and G.V. Gursky, *Molekul. Biol. (USSR)* 22, 159 (1988).
14. G.V. Gursky, V.G. Tumanyan, A.S. Zasedatelev, A.L. Zhuze, S.L. Grokhovsky and B.P. Gottikh, *Mol. Biol. Rep.* 2, 143 (1976).
15. G.V. Gursky, V.G. Tumanyan, A.S. Zasedatelev, A.L. Zhuze, S.L. Grokhovsky and B.P. Gottikh in *Nucleic Acid-Protein Recognition*, Ed. H.J. Vogel, Academic Press, New York, p. 189 (1977).
16. G.V. Gursky and A.S. Zasedatelev, *Sov. Sci. Rev. D. Physico-chem. Biol.* 5, 53 (1984).
17. A.H.-J. Wang, G. Ughetto, C.J. Quigley, T. Hakoshima, G.A. van der Marei, J.H. van Boom and A. Rich, *Science* 225, 1115 (1984).
18. Y.Y. Vengerov, T.E. Semenov, S.A. Streltsov, V.L. Makarov, A.A. Khorlin and G.V. Gursky, *FEBS Letters* 180, 81 (1985).

Date Received: July 10, 1988

Communicated by the Editor V. Ivanov